UNIVERSITY OF MINNESOTA
ST. ANTHONY FALLS HYDRAULIC LABORATORY

Project Report No. 338

Experiments on Turbulence Management Using Screens and Honeycombs

by

Cesar Farell

and

Sadek Youssef

in cooperation with
Vivek Saxena and Irsan Soemantri

Prepared for

NATIONAL SCIENCE FOUNDATION
and
STRIPPER WELL OIL OVERCHARGE GRANT,
DEPARTMENT OF ADMINISTRATION,
STATE OF MINNESOTA

December 1992
Minneapolis, Minnesota

ABSTRACT

The results of some experiments on turbulence management using combinations of honeycombs of different lengths and coarse and fine screens, carried out in highly nonuniform and turbulent flows generated in a 127-mm plexiglas pipe by an upstream blower and diffuser, are presented. The performance of the devices as single manipulators and in combination was evaluated through hot-wire measurements of the mean and rms values of the longitudinal velocities over the pipe cross section. The results show that relatively short honeycombs, preceded by a coarse screen and followed by one or more fine screens, can be used for effective management of highly nonuniform and turbulent flows.

ACKNOWLEDGEMENTS

The study reported herein is part of work done in conjunction with the design and construction of the St. Anthony Falls Atmospheric Boundary Layer Wind Tunnel, supported partially by National Science Foundation under Grants NSF/ECE-8410532 and NSF/ECE-6613554, and by the State of Minnesota under a Stripper Well Oil Overcharge Grant.

TABLE OF CONTENTS

The University of Minnesota is committed to the policy that all persons shall have equal access to its programs, facilities, and employment without regard to race religion, color, sex, national origin, handicap, age, or veteran status.

LIST OF FIGURES

1. INTRODUCTION

Traditionally, screens have been widely used to remove or create flow nonuniformities, and to control turbulence scale and intensity. Because fine wire screens are not effective in removing swirl or large scale eddy motions, and because of "singing" problems in water tunnel applications, honeycombs alone or combinations of screens and honeycombs have also been used extensively as turbulence control devices. Two important uses of these turbulence management systems are in wind and water tunnel circuits, and as conditioning devices in flow metering applications.

Low-frequency mean velocity fluctuations (unsteadiness) and spatial mean velocity nonuniformities are always present in the flow in wind and water tunnels. Spatial nonuniformities in mean velocity can be caused by inadequate design of corner vanes, by flow separations in the tunnel circuit, particularly in diffusers, or by poor fan or straightener vanes design. Unsteadiness refers generally to low-frequency fluctuations, which can be regarded as inviscid and irrotational, and are due for example to intermittent separation phenomena. Sound is also an irrotational mode of velocity fluctuations, and can be caused by mechanical vibration or fluid or fluid-elastic resonance phenomena. Excitation by unsteadiness and turbulence can produce broad band noise spectra, which may be significant unless the tunnel is fitted with sound absorbent material.

In addition to the irrotational fluctuation modes one has also the turbulent (rotational) velocity fluctuations, due to the various wakes and boundary layers in the tunnel circuit. Mean velocity nonuniformity and turbulence levels at entrance to the settling chamber can be reduced to acceptable levels in the tunnel working section by use of honeycombs, screens, and a large enough contraction ratio. Honeycombs alone are used generally in water tunnel plenums (11). It is difficult to suppress low-frequency unsteadiness without large plenum total-pressure drops, and thus one must ensure that severe separations will not be present in the circuit.

The use of screens and honeycombs as flow conditioning devices in metering applications does not appear to have been examined in detail, to the authors' knowledge. Combinations of honeycombs and screens, preferably with low overall energy loss, can be used in this case to remove flow nonuniformities and control turbulence intensity and scale to ensure the accuracy of the metering device.

In the present work, the results of some experiments on turbulence management using combinations of coarse and fine screens and honeycombs of different lengths, are presented. The investigation was carried out in highly nonuniform and turbulent flows generated in a 127-mm plexiglas pipe by an upstream blower and diffuser.

2. LITERATURE REVIEW

2.1 Honeycombs

A honeycomb has two effects on a stream: it reduces the level of the existing turbulence, and it creates additional turbulence of its own. Analyses have been developed (9, 10) for prediction of these effects, including estimates of the change in turbulence levels between a wind tunnel plenum and test section due to the intervening decay length and the effect of the tunnel contraction. Experimental verification for the analyses has been given by Robbins (11). These predictions for turbulence reduction and production by a honeycomb assume that the flow in the honeycomb cells is fully-developed turbulent. At Reynolds numbers near turbulence transition in the honeycomb cells, incidentally, higher levels of turbulence and mean velocity nonuniformity may result in the test section as a consequence of transition occurring nonuniformly across the honeycomb (11).

The work of Loehrke and Nagib (7, 8), on the other hand, was carried out with laminar honeycomb cell flow, not necessarily fully developed, with much smaller cell sizes (plastic drinking straws were used to construct the honeycomb). Under these conditions, the thwarting of the transverse velocity components by the cell walls was particularly effective. The results suggest in fact that the major part of this suppression occurred within a short distance from the leading edge of the straws, and thus that much shorter cell lengths than required to reach fully developed laminar flow can be used in design (5 to 10 cell diameters). A major finding of this work was the suppression effect that an adequately placed screen had on the honeycomb wake shear layer instability responsible for downstream turbulence generation. The screen (wire diameter 0.13 mm, open area ratio 0.72) was placed upstream of the point where the instability started to grow rapidly, so that the smaller dissipative scales of the screen replaced the larger scales of the honeycomb. The recommended distance is less than 5 cell sizes. The importance of matching the scales of coupled turbulence management devices has been documented by Tan-atichat et al. (16).

2.2 Screens

Classical papers on the characteristics of damping screens are those of Dryden and Schubauer (4), Schubauer et al. (14), and Taylor and Batchelor (17). A comprehensive list of other earlier investigations and a concise review of the problem are given by Loehrke and Nagib (7). The flow through a screen can be characterized as subcritical or supercritical depending on the fluctuation levels immediately downstream of the screen. In the subcritical regime, at small Re, no eddies are shed by the screen, and the levels are lower than those in the oncoming stream. For larger

Re, in the supercritical regime, the levels are far above those in the oncoming stream, but decrease rapidly with distance and reach values significantly below the original free-stream turbulence intensity. The critical Re depends on the screen solidity ratio (14). Tan-atichat et al. (16) recommend that screens not be operated at subcritical Re because the performance of the screen is strongly dependent on the free-stream velocity. While subcritical screens have been used in wind tunnels with no apparent detrimental effects on the tunnel performance (2), the velocity dependence must obviously be kept in mind for design purposes. Near the critical Re, on the other hand, the damping characteristics of the screen can change abruptly with small changes in flow conditions, and this situation must be avoided.

To characterize a flow management device, turbulence energy reduction factors can be defined as the ratios of downstream to upstream mean square values at the position of the device. The downstream values must be obtained by back extrapolation from a downstream location where the local effects of the device are no longer felt, while the upstream values are simply those measured in the undisturbed stream. Alternately, ratios of mean square values at a given downstream section, with and without the device, can be used. Reduction factors for spatial mean velocity variations can likewise be defined. Existing theories lump screen characteristics in two experimental coefficients: the pressure drop coefficient, K, and the refraction coefficient, α, the latter defined as the ratio of the angles that the downstream and upstream mean flow directions make with the normal to the screen. Various available theories and experimental data show only limited agreement, and consideration of the detailed mechanisms of both turbulence generation and suppression by the screen may be necessary to improve the predictions (7).

Plots of the longitudinal (μ) and lateral (ν) turbulence energy reduction factors predicted by Taylor and Batchelor's theory (17) are given in Corrsin (3) and Batchelor (1), assuming for the refraction coefficient the empirical expressions $\alpha = 1.1/\sqrt{(1+K)}$ for $K > 0.7$, and $\alpha = (8-K)/(8+K)$ for $K < 0.7$ (4). The data of Townsend (18) are also shown. The theory predicts too great a degree of anisotropy downstream from the screen, but the total energy reduction given by $(\mu+2\nu)$ appears to be predicted more accurately by it. As Corrsin (3) has shown, the Taylor-Batchelor turbulence reduction factors μ and ν are approximately equal to the energy reduction factors for spatial mean velocity nonuniformities (also given by the Taylor-Batchelor theory as a particular case of the Fourier decomposition) if use is made of the aforementioned empirical relations between α nd K. Under these conditions, $\sqrt{\nu} = \alpha = 1.1/\sqrt{(1+K)}$ for $K > 0.7$. This particular result, with 1.0 in the numerator instead of 1.1, was experimentally obtained by Schubauer et al. (14) and Scheiman (13). Although there is then some agreement in the results for lateral component reduction, this is not the case for the data and theories for the longitudinal component. In regard to the Taylor-Batchelor theory, questionable assumptions (in

particular downstream of screens operating in the supercritical regime) are that the wake turbulence produced by the screen wires can be neglected and that the turbulence intensities are small.

2.3 Honeycomb-screen combinations

Measurements of the turbulence characteristics behind combinations of screens and honeycombs have been carried out by Scheiman (13). The length-to-diameter ratio of the honeycombs was chosen as 6 or 8 on the basis of the laminar cell flow results of Loehrke and Nagib (7,8) cited earlier. But the cell Re of these experiments are in the transition range or higher (the precise values of the velocity for the results shown in Figs. 11 through 14 of this reference are not given) and, furthermore, the first screen behind the honeycomb was placed so that the honeycomb turbulence was almost completely decayed before encountering it. These data are essentially then different from those of Loehrke and Nagib. In general, the turbulence reduction of a screen when placed downstream of a honeycomb was found to be much better than that for the screen alone. There appear to be some inconsistencies in the data, however, which require elucidation for comparison with other results.

Results of an exploratory examination of the mechanism of turbulence generation by a honeycomb and a fine screen have been reported by Xia et al. (19). The honeycomb and screen were tested as single devices and in combination, with the screen at various separation distances behind the honeycomb. Velocity fluctuation spectra measured downstream of the honeycomb disclosed the presence of organized flow structures, which persisted for some distance and were particularly well defined for the smaller cell Reynolds numbers tested. The distance at which the structures disappeared increased with decreasing Reynolds number and was about 11 d for $Ud/\nu = 1{,}640$ (d = cell diameter, U = average cross sectional velocity). No organized motion was observed for $Ud/\nu > 3{,}900$. For $Ud/\nu < 3{,}900$, installation of the screen immediately downstream of the honeycomb was effective in thwarting the instability growth responsible for the organized motion. The associated spectral peaks either disappeared altogether or became unimportant a short distance downstream from the screen, depending on the Reynolds number, with a concomitant large reduction in turbulence intensity and a shifting of the intensity maxima toward the screen.

3. INSTRUMENTATION AND EXPERIMENTAL PROCEDURE

A plexiglas pipe with internal diameter D = 5 in (127 mm) was used to study the effect of honeycombs and screens on the air flow produced by an upstream blower. A 66-cm long diffuser with an included angle of 5 degrees connected the 70-mm-diameter fan outlet to the plexiglas pipe. Three honeycombs, with lengths l = 2 in (50.8 mm, HC2), 5 in (127 mm, HC5), and 10 in (254 mm, HC10), were constructed using plastic drinking straws with internal diameter d = 5.95 mm. The honeycomb pressure drop coefficients, $K = \Delta p / (\frac{1}{2}\rho U^2)$, were estimated respectively as 0.90, 1.85, and 2.9 at a pipe $Re_D = UD/\nu$ = 51,300 (U = 6.1 m/s, Re_{cell}= 2,730). Here U = average cross sectional velocity and $Re_{cell} = (1/\beta)Re_d = (1/\beta)(Ud/\nu)$ = honeycomb cell flow Reynolds number. The pressure loss estimates were based on limited measurements carried out with nonuniform honeycomb approach flows and may be in error by ± 15 percent. The value of K and the accuracy of the experimental determination of the average velocity U depend strongly on the characteristics of the oncoming flow, and additional measurements will be necessary to improve the accuracy of the estimates. At Re_D = 30,700 (U = 3.66 m/s, Re_{cell} = 1,640) the measured pressure drop coefficients were respectively 1.4 (HC2), 3.1 (HC5), and 4.8 (HC10). The open-area ratio of the honeycombs was β = 0.88.

One coarse screen (CS, 3 wires/in, mesh size M = 8.47 mm, wire diameter d_w = 2.03 mm, β = 0.578) and two fine screens (FS1, 16 wires/in, M = 1.59 mm, d_w = 0.254 mm, β = 0.706; and FS2, 20 wires/in, M = 1.27 mm, d_w = 0.229 mm, β = 0.672) were used in the investigation. The coarse screen was installed always before the honeycomb. Estimated K values at pipe Re_D = 51,300 (U = 6.1 m/s) were 0.95 for CS (wire diameter Reynolds number Re_w = 820), 0.70 for FS1 (Re_w = 103), and 0.85 for FS2 (Re_w = 93). The corresponding K values for Re_D = 30,700 were 1.02 (CS, Re_w = 492), 0.86 (FS1, Re_w = 62), and 1.02 (FS2, Re_w = 56). On the basis of Schubauer et al.'s relationship (14) between critical Re and β, all screens operated in the supercritical regime for pipe Re_D > 30,700, although FS2 at Re_w = 56 is close to the subcritical boundary.

The general arrangement of screens and honeycombs is shown in Fig. 1. For the experiments with honeycombs HC5 and HC10, the input and output sections where the velocity distributions were measured are shown in Figs. 1 b) and 1 c). These sections were located before and after the honeycomb-fine screen combinations, 23 in (584.2 mm) apart, except when HC10 was tested, in which case the distance was increased to 27 1/16 in (687.4 mm). For the experiments without screen CS, the input and output sections were at the same positions, with the end of the diffuser brought 206.4 mm closer. Velocity distributions with honeycomb HC2 in the pipe were measured at several distances X from the flange section where the coarse screen was installed. The origin for the distance x = X - 279.4 mm was at

the end of the honeycomb. Figures 2 and 3 show photographs of the experimental arrangement, one of the honeycombs, and screen FS1.

Longitudinal velocities were measured across several pipe cross sections using a TSI model 1054A hot-wire anemometer. The rms values of the fluctuations were obtained by means of a Fluke digital multimeter, model 8520A, using an averaging time of 30 seconds. In the experiments with honeycomb HC2 in the new facility a Hewlett-Packard digital multimeter, model 3457A, was used, with a 40-second averaging time. Other equipment included a manometer with a resolution of 0.025 mm of gage fluid, an oscilloscope for signal monitoring, and a Hewlett-Packard digital signal analyzer, model 35660A. Additional descriptions and photographs of the experimental setup can be found in Refs. 12 and 15.

4. PRESENTATION OF RESULTS

Selected representative profiles of dimensionless mean velocities, $\bar{u}/U$, and rms turbulence intensities, $u'/\bar{u}$, are shown in Figs. 4 through 14. In addition to the notation introduced for honeycombs and screens, the following has also been used for brevity: E, empty pipe; W, combination of coarse screen CS, honeycomb HC5, and fine screen FS1; W2, combination of CS, HC2, FS1, and FS2; V, vertical and H, horizontal, traverses; I, input and O, output, sections. Only results for the larger Reynolds number investigated (Re_D = 51,300, Re_{cell} = 2,730) are presented here. Some results for laminar honeycomb cell flow (Re_D = 30,700, Re_{cell} = 1,640) are reported in Refs. 12 and 19.

4.1 Experiments with honeycombs HC5 and HC10

For the pipe without manipulators (see Figs. 4 and 5, E) the profiles were rather nonuniform and asymmetric. A longitudinal swirling motion appeared to be present. Output turbulence intensities were of the order of 9 to 10 percent near the pipe centerline, while input intensities were much higher, around 16 percent. Comparison of the input profiles shown in Fig. 4 with input profiles measured after installation of other manipulators (e.g., profile CS,V,I in Fig. 4 and the vertical input profiles CS+HC5 in Fig. 7, and W in Fig. 9; other comparisons, including empty pipe profiles, in Ref. 12) showed differences in mean velocities and turbulence intensities of at most 5 and 10 percent, respectively, with smaller differences near the pipe centerline. Given the high turbulence levels, the strong cross-sectional nonuniformity of the flow, and the inherent errors in hot-wire measurements under these conditions (see e.g. Ref. 5) it was concluded that the presence of the manipulators affected only slightly, if at all, the oncoming flow as produced by the blower.

Figure 4 presents also the vertical velocity distributions in the pipe with screen CS installed. The comparable vertical and horizontal input profiles for combinations CS+HC5 and W are shown respectively in Figs. 7 and 9. (The input measurement section was downstream from screen CS in all cases.) All E and CS profiles showed significant asymmetry. There was considerable difference in the input section mean velocity profiles with and without the coarse screen. This is not the case for the output vertical mean profiles shown in Fig. 4, but one would expect the output horizontal profile with CS installed, not measured, to be quite different from the corresponding empty pipe profile. The CS results suggested again the presence of longitudinal swirl in the pipe. The input turbulence intensities showed a marked decrease after installation of the screen. The change in output section intensities was less but still significant.

The performance of honeycombs HC5 and HC10 as single manipulators is depicted in Figs. 5 and 6. The empty pipe output profiles are shown in Fig. 5 for comparison. As discussed earlier, the E input profiles of Fig. 4 can be taken to depict the input profiles to HC5 and HC10. Comparison of input and output profiles suggested that the swirling motion in the pipe was reduced by both honeycombs. (Measurements at a few points at other longitudinal locations supported also this conclusion.) On the other hand, Figs. 5 and 6 show no significant improvement in the uniformity of the mean velocity profiles over the empty pipe profiles: for example, the momentum defect in the vertical input profile (for negative y) is still present in both the HC5 and HC10 output profiles. The output turbulence intensities were lower, however, with the honeycombs in the pipe. The magnitude was about the same for both, with HC10 showing somewhat better uniformity (see Fig. 6).

The effect of adding screen CS on the performance of honeycomb HC5 is shown in Fig. 7. Both input and output profiles are shown, together with the output profiles for HC5 alone. The performance of the honeycomb was improved by the addition of the coarse screen. This was also true for honeycomb HC10, but there was no advantage in using the longer over the shorter honeycomb, and the remainder of the tests was carried out with HC5.

The output profiles obtained with screen FS1 placed downstream of honeycomb HC5 a distance equal to 5 times the honeycomb cell internal diameter are shown in Fig. 8, together with the profiles for HC5 alone. Addition of this screen resulted in somewhat better uniformity in the output profiles, and lower turbulence intensities. The effect of adding screen CS to HC5 and FS1 to form combination W is shown in Figs. 9 and 10. Input and output profiles are shown in Fig.9, and a comparison with output profiles for HC5 and HC5+FS1 is shown in Fig.10. There was a distinct improvement in the uniformity of the $\bar{u}/U$ and $u'/\bar{u}$ profiles for combination W, and the turbulence intensities became significantly lower.

With individual loss coefficients of 1.85 for HC5, 0.95 for CS, and 0.70 for FS1, the overall loss coefficient of the W combination was K = 3.50. The output mean velocities at distances y, z less than 80 percent of the pipe radius were within ±5 percent from their mean value, while the turbulence levels were between 2.5 percent (near the pipe centerline) and 3.5 percent. Under these conditions, it would be possible to achieve further improvement in uniformity and reduction in turbulence levels through addition of more fine screens, at the expense of a larger pressure loss. On the other hand, comparison of the HC5 and HC10 results showed that, at least under the conditions of the experiments, there was no advantage to be gained by using the longer honeycomb. It was then decided to investigate the performance of the even shorter honeycomb HC2 (l/d = 8.53) which, with a lower K = 0.95, would allow the use of one additional screen for about the same overall K.

4.2 Experiments using honeycomb HC2

The centrifugal blower used to produce the flow had to be replaced when the facility was moved to another building, midway through the experiments with honeycomb HC2. Figure 11 shows mean velocity profiles measured in the old facility at X = 19 in (482.6 mm) for combination W2 (CS+HC2+FS1+FS2, overall K = 3.40), together with the empty pipe profiles. The corresponding rms fluctuations are not shown because of possible instrument errors in the measurements involving the HC2 honeycomb in the old facility, which were corrected at the time the blower was replaced. The W2 profiles in Fig. 11 show significant improvement in uniformity in comparison with the profiles for combination W (CS+HC5+FS1, overall K = 3.50) in Fig. 10. The mean velocity values in Fig. 11 at distances y, z less than 80 percent of the pipe radius are within ±1.5 percent from their average over this portion of the pipe cross section.

Replacement of the blower changed the oncoming flow conditions. Velocity profiles for the pipe without manipulators, measured in the new installation, are given in Figs. 12 to 14 at five cross sections, from X = 4 in (101.6 mm) to X = 35 in (889 mm). As the E results in these figures show, the nonuniformity and asymmetry of the empty pipe flow were much more pronounced in the new installation. The mean velocity profiles suggest also that a longitudinal swirling motion was present in the pipe without manipulators. Turbulence intensities near the pipe centerline were around 17 percent at X = 4 in (101.6 mm), 12 percent at X = 19 in (482.6 mm), and 10 percent at X = 35 in (889 mm). Comparison of E profiles measured at a given cross section, with profiles measured at the same location after installation of an additional length of pipe downstream from it, showed differences in mean velocities and turbulence intensities of at most 2 and 4 percent, respectively, confirming the earlier conclusion that the presence of manipulators (or of an additional pipe length) affected only slightly if at all the oncoming flow as produced by the blower. Figure 12 shows also for reference the profiles with screen CS only in the pipe, at X = 4 in (101.6 mm) and X = 9 in (228.6 mm).

A comparison of the profiles produced at X = 19 in (482.6 mm) by manipulator combinations CS+HC2 and W2 (CS+HC2+FS1+FS2) is shown in Fig. 13. The W2 mean velocities in this figure, at distances y, z less than 80 percent of the pipe radius, are within 3.8 percent from their average. For y, z less than 40 percent of the pipe radius, the velocities are within 2.1 percent from their average. The deviations are larger than those measured for the same combination in the old installation, but the nonuniformity and asymmetry of the oncoming flow were much more pronounced in the new facility (cf. Figs. 4, 11 and 12, 13).

5. DISCUSSION

5.1 Mean velocity profiles

The large momentum defect present in the flow in the pipe without manipulators for $y < 0$ (Fig. 4) was still present in the output profiles for honeycombs HC5 and HC10 (Figs. 5 and 6), which produced only a slight improvement in flow uniformity. The performance of HC10 was just slightly better than that of HC5. One can see in Fig. 5 that HC5 actually preserved to a considerable extent the shape of the input $\bar{u}$ profiles (E, Fig. 4). The honeycombs, on the other hand, were effective as expected in reducing the pipe swirl. The output profiles without manipulators (O, Fig. 5) show the evolution of the pipe flow itself. The $\bar{u}$ profiles in the empty pipe became less nonuniform and the rms turbulence intensities u' decreased with distance downstream.

These results suggest that the energy losses in the honeycombs cells were not large enough to produce significant flow uniformization through redistribution of the oncoming flow. On the other hand, the channeling of the flow by the cells prevented the momentum exchange that would otherwise result from the dynamics of the energy containing, large eddies of the approach flow. The scale of these eddies, of the order of, say, the pipe radius, is the relevant length scale in dealing with the interaction of the turbulence with the mean flow. The large oncoming flow eddies are responsible for the relative decrease in the nonuniformity of the $\bar{u}$ profiles as the flow proceeds along the empty pipe, while the reduction in turbulence energy results from the cascade process of generation of smaller eddy scales and the subsequent dissipation of energy toward the small scale end of the spectrum.

Installation of screen CS in the pipe resulted in a modification of the eddy structure and a considerable reduction in flow nonuniformity and turbulence levels (cf. Fig. 4, profiles E,I and CS,I, and Fig. 9, profiles W,I). The mesh size of screen CS (8.47 mm) was sufficiently large to enhance, via the large-scale eddy structure it produced, the interaction of the turbulence with the incoming mean flow inhomogeneities. (We note here for the purpose of this comparison that the input section with screen CS in the pipe was 206.4 mm downstream of the input section in the empty pipe, where CS was actually installed). Comparison of data taken in the new facility at $X = 4$ in (101.6 mm), with and without screen CS at $X = 0$, confirmed the significant effect of this screen on the flow (cf. Fig. 12). The choice of screen mesh size and diameter is critical to ensure the correct performance of a screen. A screen may actually be very inefficient in reducing mean flow nonuniformity and turbulence levels if the oncoming flow contains gross inhomogeneities and large scale turbulence and the screen dimensions are much smaller than the size of the oncoming flow features (16). On the other hand, screens are generally not

effective in reducing large scale swirling, and indeed longitudinal swirl was still detected in the pipe with screen CS installed.

The preceding discussion suggests that in order to use a relatively short honeycomb to reduce large scale swirling motions and turbulence levels, it is best to install a coarse screen upstream from it so that the flow reaching the honeycomb cells is as uniform as possible. The $\bar{u}$ data for honeycomb HC5 (Fig. 7, curves HC5 and CS+HC5; Fig. 10, curves HC5+FS and W) show the improvement in performance when CS is added to the system. The performance of CS+HC10 (results not shown) was very close to that of CS+HC5. For the shorter honeycomb HC2, under the rather nonuniform approach flow conditions in the new facility, there was only a small reduction on $\bar{u}$ nonuniformity due to the honeycomb itself, as illustrated by a comparison of the coarse screen profiles in Fig. 12 at X = 9 in (228.6 mm), corresponding to the position of the honeycomb inlet, and profiles CS+HC2 in Fig. 13 at X = 19 in (482.6 mm). On the other hand, the reduction in turbulence intensity due to honeycomb HC2 and the intervening length of pipe between the two positions was considerable, from about 7 to 4 percent.

5.2 Velocity fluctuation profiles

To summarize the rms velocity fluctuation data included in Figs. 4 through 13, the average and the standard deviation of the $u'/\bar{u}$ values in the 55-mm-diameter center portion of the pipe have been calculated for each manipulator combination and are presented in Fig. 15. The results are plotted for convenience along four vertical lines. The first and second lines contain the output section averages and standard deviations for the experiments in the old facility, respectively without and with screen CS, with honeycombs HC5 or HC10 as one of the manipulators. The third and fourth lines contain the averages and standard deviations at X = 19 in (482.6 mm, x = 203.2 mm) and X = 4 in (101.6 mm) for experiments in the new facility related to the use of honeycomb HC2 as a manipulator.

Both with and without the upstream screen CS, the performance of honeycombs HC5 and HC10 was about the same. The turbulence intensity was reduced by a factor between 1.7 and 1.8 relative to the intensity at the same section without the honeycomb. Without the coarse screen, the cross section profiles were slightly more uniform and the reduction factor slightly larger for HC10 (see Fig. 15 b). The results of Lumley and McMahon (10) can be applied to honeycomb HC10 since the cell flow is fully developed turbulent as defined in their Fig. 2. Assuming an integral length scale L $\approx$ 75 mm for the incoming turbulence, we have L/l $\approx$ 0.30, and the rms turbulence reduction factor obtained from Fig. 1 of Ref. (10) is $\sqrt{\eta}$ $\approx$ 0.16 ($\sqrt{\eta}$ varies between about 0.165 for K = 2.2 and 0.15 for K = 2.9). Adding the contributions from the residual turbulence and the turbulence generated by the honeycomb (330.2 mm downstream from it) one gets $u'/\bar{u} \approx 0.03$ for HC10 in the empty pipe (input section

turbulence intensity $u'/\bar{u} \approx 0.16$, see Fig. 4), and $u'/\bar{u} \approx 0.02$ for HC10 downstream of CS (input $u'/\bar{u} \approx 0.09$, see Fig. 7). The measured values (about the same as the values for HC5) are about 80 percent larger. One can conjecture that the rather nonuniform nature of the flow may be responsible for this difference, resulting perhaps in nonnegligible turbulence production by the mean flow. Elucidation of these results requires however further investigation.

The results for the shorter honeycomb HC2 showed a large decrease in turbulence intensity at X = 19 in (482.6 mm, x = 8 in = 203.2 mm) due to installation of CS+HC2 in the pipe, from $u'/\bar{u} \approx 0.12$ to $u'/\bar{u} \approx 0.04$ (see Fig. 13). (Measurements with HC2 alone in the pipe were not carried out in view of the results for the longer honeycombs.) The empty pipe flow in the new installation contained gross inhomogeneities (still present to a considerable extent at x = 203.2 mm after installation of CS+HC2, see Fig. 13) and large scale turbulence and swirl. The addition of fine screens downstream of honeycomb HC2 served then not only to reduce further the turbulence intensities but also, through improvement in the flow uniformity, to prevent the generation of additional turbulence through nonzero mean flow gradients.

The turbulence energy reduction factors of screen CS relative to the empty pipe flow, of screen FS1 downstream of HC5 and CS+HC5, and of screens FS1 and FS2 downstream of CS+HC2, can be compared with the existing theories and measurements reviewed briefly in Section 2.2. For this comparison, values of the turbulence energy reduction factors μ and ν were obtained by three methods: the expressions $\sqrt{\mu} = 1/(1+K)$ and $\sqrt{\nu} = 1/\sqrt{(1+K)}$ (method 1), Taylor and Batchelor's theory (method 2), and the data of Townsend plotted in Ref. (1) together with Taylor and Batchelor's theoretical results (method 3). The reduction in total energy given by $(\mu+2\nu)$ and the reduction factor $R = \sqrt{(\mu+2\nu)}$ were then calculated. Inspite of the differences in the predicted individual values of μ and ν, the estimates for total energy reduction provided by the three methods were actually fairly close. The estimates R_e were, respectively for methods 1, 2, and 3: for CS, 0.66, 0.68, and 0.63 (average $R_e \approx 0.66 \pm 0.03$); for FS1, 0.71, 0.72, and 0.69 (average $R_e \approx 0.71 \pm 0.02$); and for FS2, 0.68, 0.70, and 0.66 (average $R_e \approx 0.68 \pm 0.02$). These estimates can be correlated with the measurements depicted in Fig. 15 as follows.

For screen CS, comparison of the relative intensity values with and without the screen at the input and output sections in the old installation gave a measured reduction factor R_m between 0.70 and 0.75. This estimate is subject to some error, firstly because the longitudinal positions of the output and input sections are different in both cases and the comparison required interpolation, secondly because only vertical profiles were measured at the output section with CS installed, and both the $\bar{u}/U$ and $u'/\bar{u}$ distributions were rather nonuniform. In the new installation, the reduction

factors at X = 4 in (101.6 mm) and X = 9 in (228.6 mm), obtained by division of the relative intensity values with and without the screen, were about the same, approximately equal to 0.53. This large reduction is likely due to the rather disturbed nature of the approach flow and the direct effect that screen CS, placed at the exit section of the diffuser, had on the diffuser flow.

For screen FS1 (placed 27 mm downstream from honeycomb HC5) the measured reduction factor, R_m, can be obtained by direct division of the results in Fig. 15, since these represent measurements at the same cross section (179.4 mm downstream from the screen), with and without FS1. One gets $R_m = 0.79$ with screen CS in the system and $R_m = 0.73$ with screen CS removed. While the last value is close to the average estimate of 0.71, the reason for the smaller turbulence reduction in the case of the more uniform flow with screen CS in the pipe is not clear.

Finally, for screens FS1 and FS2 together, the measurements in the new installation give $R_m \approx 0.51$ at a cross section 76.2 mm (60 M) downstream of the position of FS2 (179.4 mm downstream of FS1), about 6 percent larger than the product of the average estimates $(0.71)(0.68) \approx 0.48$. Multiplying on the other hand $R_m \approx 0.79$ for screen FS1 by the estimate 0.68 for FS2 yields about 0.54, somewhat larger than the measured $R_m \approx 0.51$. It is noted here also that measurements in the old facility appeared to show that the turbulence reduction due to both screens FS1 and FS2 was unchanged by a 127 mm downstream shift of both screens. This last result would imply that the separation between honeycomb and first screen is not critical in the case of turbulent honeycomb cell flow, contrary to the case of laminar cell flow (7, 8; see also Ref. 19). Some of these questions are the object of a current investigation, with the results to be reported separately.

6. CONCLUSIONS

The performance of combination W2 (the shorter honeycomb HC2 and screens CS, FS1, and FS2; total K ≈ 3.4) may be satisfactory for many applications, in particular given the disturbed nature of the oncoming flow in the new facility. The $\bar{u}$ values measured in the old and new facilities over the central core of the pipe cross section, at distances y, z less than 80 percent of the pipe radius, were within 1.5 and 3.8 percent, respectively, from their central core averages. The smallness of these deviations allows for further improvement in flow uniformity, if necessary, through addition of one or more fine screens, at the expense of an increase in K of about 0.75 per screen. Relative turbulence intensities were reduced from about 12 to 2 percent by this combination. Questions remain regarding optimum honeycomb length, screen sizes, and manipulator spacings, all likely dependent on the quality of the oncoming flow. The effect of approach flow characteristics on manipulator performance requires in particular further investigation.

Both with and without the upstream screen CS, the performance of honeycombs HC5 and HC10 as single manipulators was about equal. The large momentum defect present in the flow in the empty pipe was still present in the output profiles for both honeycombs, which produced only a slight improvement in flow uniformity. The honeycombs, on the other hand, were effective in reducing pipe swirl. The turbulence intensity was reduced by a factor between 1.7 and 1.8 relative to the intensity at the same section without either honeycomb. Application of Lumley and McMahon's (6) theory to honeycomb HC10 resulted in much smaller turbulence intensities than the measured values.

Screen energy reduction factors estimated by existing theories and data showed some differences with the measured values, of the order of 10 percent, due likely to the dependence of a screen performance on approach flow conditions. The estimates reviewed can be used as a first approximation for screen selection. Finally, the results and analysis suggest that in order to use a relatively short honeycomb to reduce large scale swirling motions and turbulence levels, it is best to install an upstream coarse screen so that the flow reaching the honeycomb is as uniform as possible.

7. REFERENCES

1. Batchelor, G.K., 1967, The Theory of Homogeneous Turbulence, Cambridge University Press.

2. Cermak, J.E., 1981, "Wind Tunnel Design for Physical Modeling of Atmospheric Boundary Layers," J. Eng. Mech., ASCE, Vol. 107, pp. 623-642.

3. Corrsin, S., 1963, "Turbulence: Experimental Methods," Handbuch der Physik, Vol. 8, No. 2.

4. Dryden, H. L., and Schubauer, G. B., 1947, "The Use of Damping Screens for the Reduction of Wind Tunnel Turbulence," J. Aeronautical Sciences, Vol. 14, pp. 221-228.

5. Fingerson, L. M., and Freymuth, P., 1983, "Thermal Anemometers," Ch. 4, Fluid Mechanics Measurements, R. J. Goldstein, Ed., Hemisphere Pub. Corp.

6. Laws, E.M. and Livesey, J.L., 1978, "Flow Through Screens," Annual Reviews of Fluid Mechanics, Vol. 10, pp. 247-266.

7. Loehrke, R.I., and Nagib, H.M., 1972, "Experiments on Management of Free-Stream Turbulence," AGARD Report No. 598.

8. Loehrke, R.I., and Nagib, H.M., 1976, "Control of Free Stream Turbulence by Means of Honeycombs: A Balance Between Suppression and Generation," J. Fluids Eng., Vol. 98, pp. 342-353.

9. Lumley, J.L., 1964, "Passage of a Turbulent Stream Through Honeycomb of Large Length-to-Diameter Ratio," J. Basic Eng., Trans. ASME, Series D, Vol. 86, pp. 218-220.

10. Lumley, J.L., and McMahon, J.F., 1967, "Reducing Water Tunnel Turbulence by Means of a Honeycomb," J. Basic Eng., Trans. ASME, Series D, Vol. 89, pp. 764-770.

11. Robbins, Basil E., 1978, "Water Tunnel Turbulence Measurements Behind a Honeycomb," J. Hydronautics, Vol. 12, pp. 122-128.

12. Saxena, V., 1989, "Reduction of Turbulence in a 5-inch Conduit Using Honeycombs and Screens," M.S. Thesis, Univ. of Minnesota.

13. Scheiman, J., 1981, "Comparison of Experimental and Theoretical Turbulence Reduction Characteristics for Screens, Honeycomb, and Honeycomb-Screen Combinations," NASA TP 1958.

14. Schubauer, G.B., Spangenberg, W.G. and Klebanoff, P.S., 1950, "Aerodynamic Characteristics of Damping Screens," NACA TN 2001.

15. Soemantri, I., 1990, "On the Use of Short-Length Honeycombs for Turbulence Management," M.S. Thesis, Univ. of Minnesota.

16. Tan-atichat, J., Nagib, H.M., and Loehrke, R. I., 1982, "Interaction of Free-Stream Turbulence with Screens and Grids: A Balance Between Turbulence Scales," J. Fluid Mech., Vol. 114, pp. 501-528.

17. Taylor, G.I. and Batchelor, G.K., 1949, "The Effect of Wire Gauze on Small Disturbances in a Uniform Stream," Quart. J. Mech. and Applied Math., Vol. 2, pp. 1-29.

18. Townsend, A.A., 1951, "The Passage of Turbulence Through Wire Gauzes," Quart. J. Mech. and Applied Math., Vol. 4, p. 308.

19. Xia, L., Farell, C., and Kavanagh, P., 1990, "Experimental Investigation of the Unsteady Flow Behind Screens and Honeycombs," Proc., 36th International Instrumentation Symp., Instrument Soc. of America, pp. 367-376.

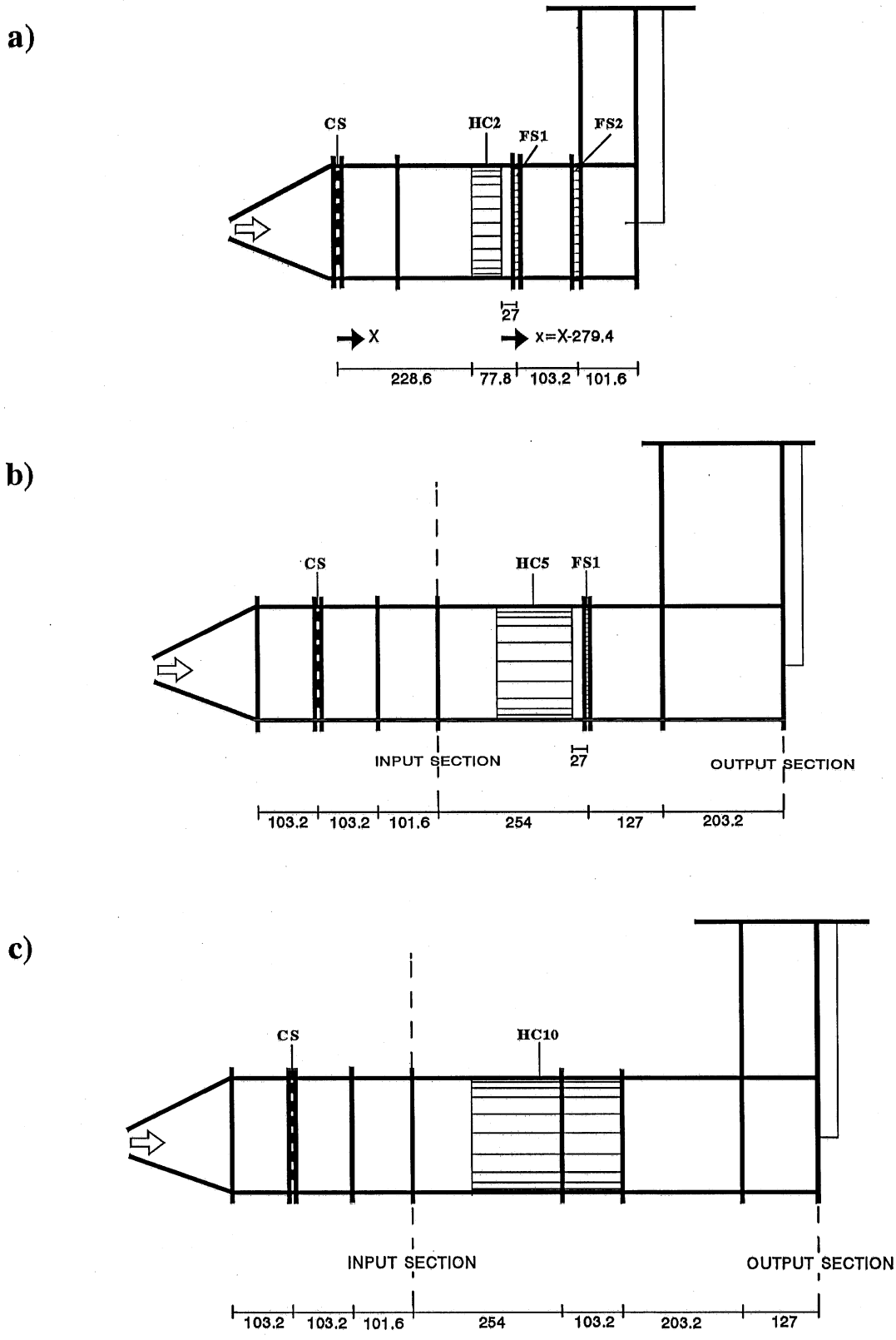

Fig. 1 General arrangement of screens and honeycombs (dimensions in mm)

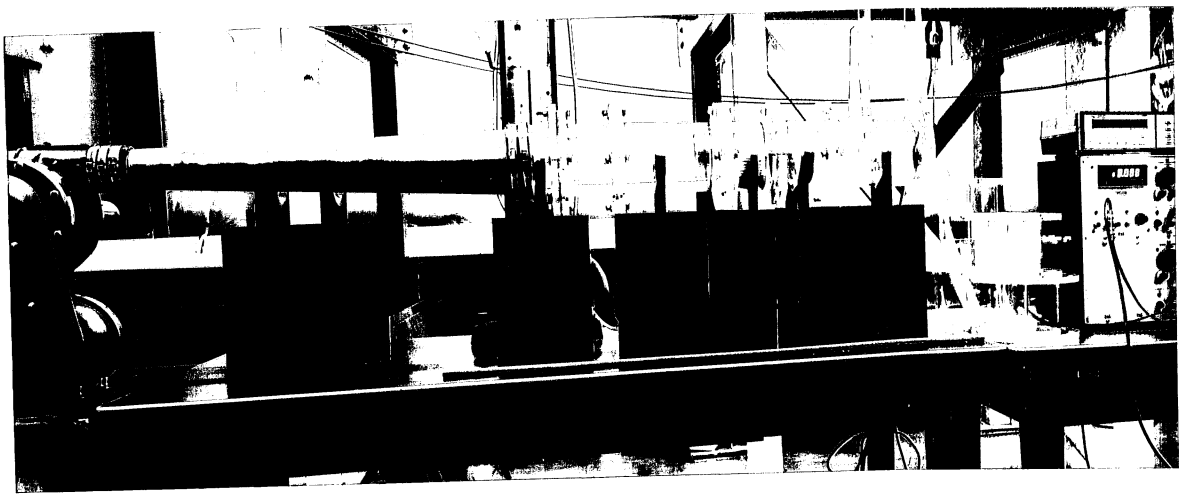

Fig. 2 View of experimental set-up.

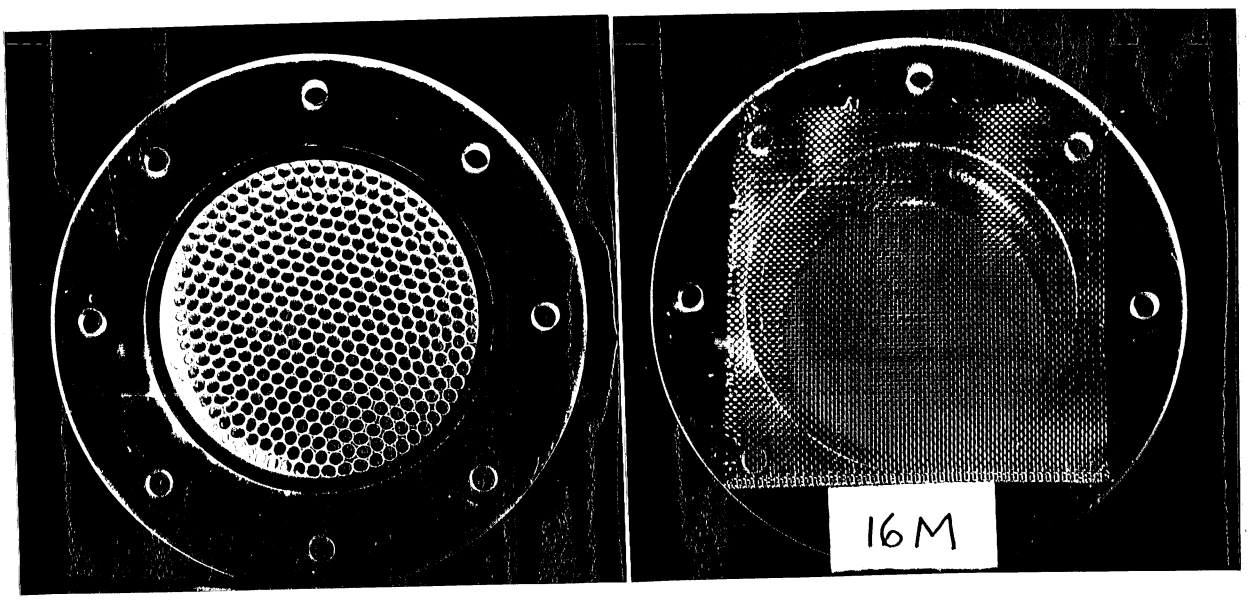

Fig. 3 View of honeycomb HC2 and screen FS1.

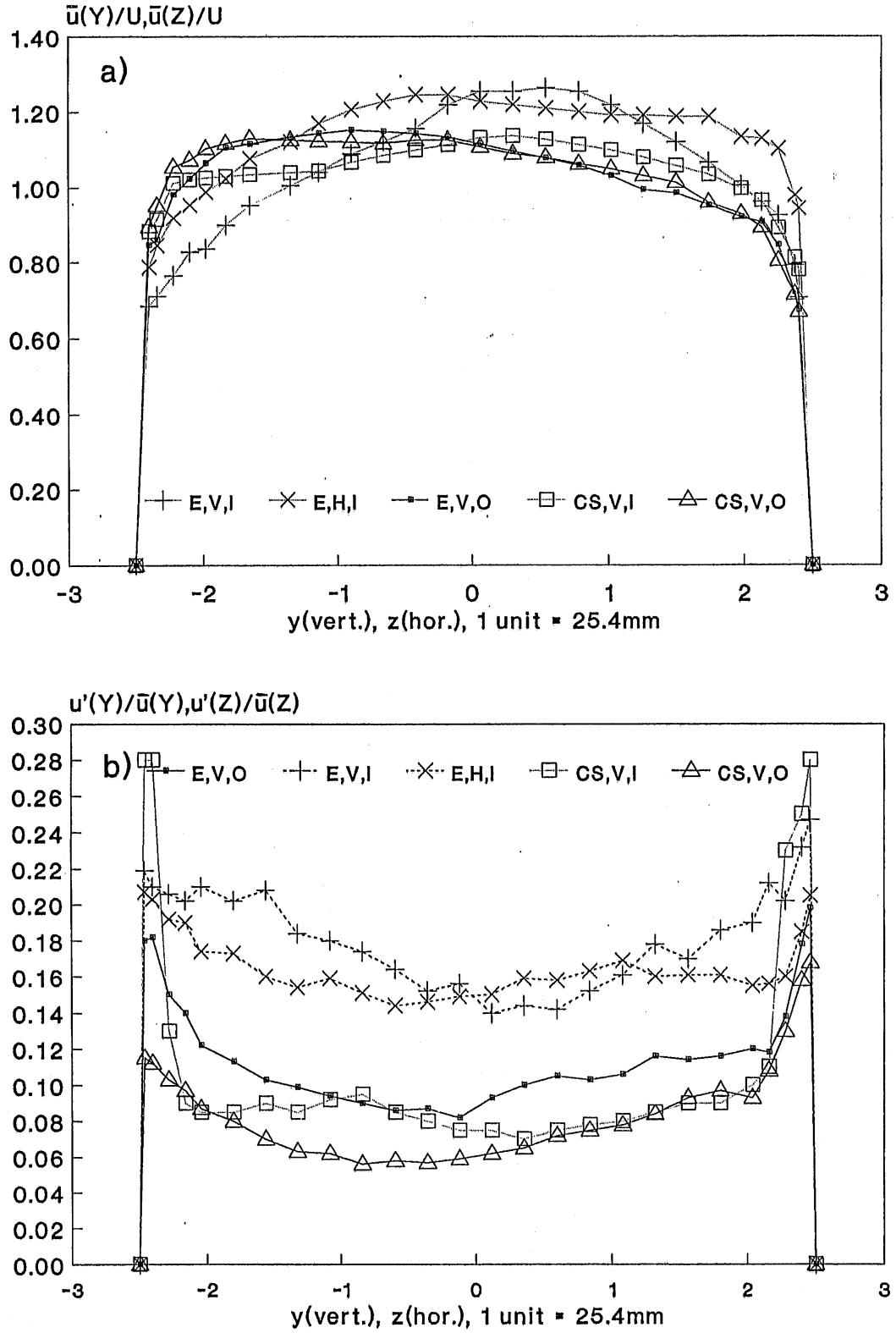

Fig. 4 a) Mean velocity and b) Velocity fluctuation profiles in empty pipe (E) and in pipe with coarse screen (CS). (H, horizontal traverse; V, vertical traverse; I, input section; O, output section).

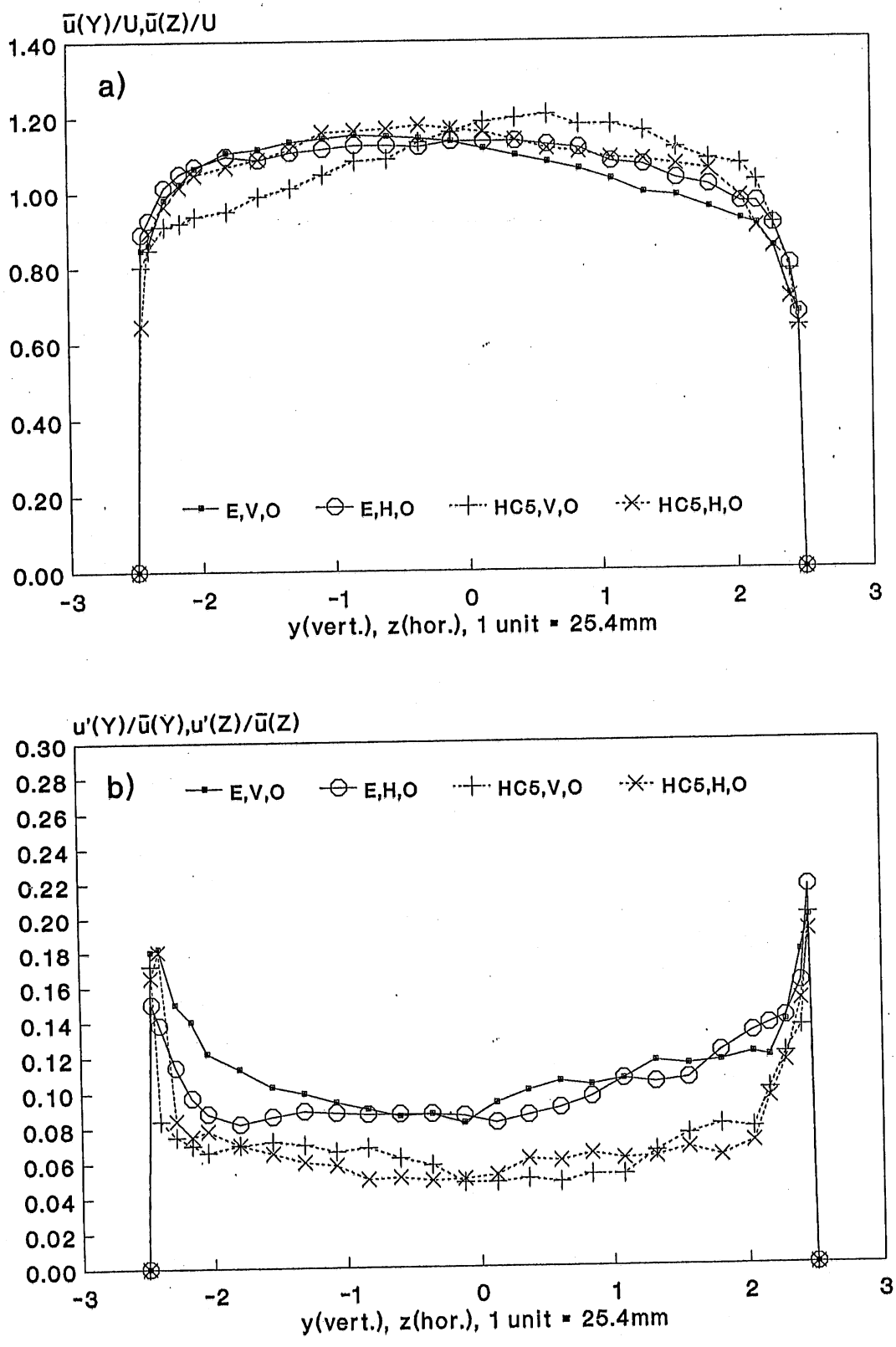

Fig. 5 a) Mean velocity and b) Velocity fluctuation profiles in empty pipe (E) and in pipe with honeycomb HC5. Other symbols as in figure 4.

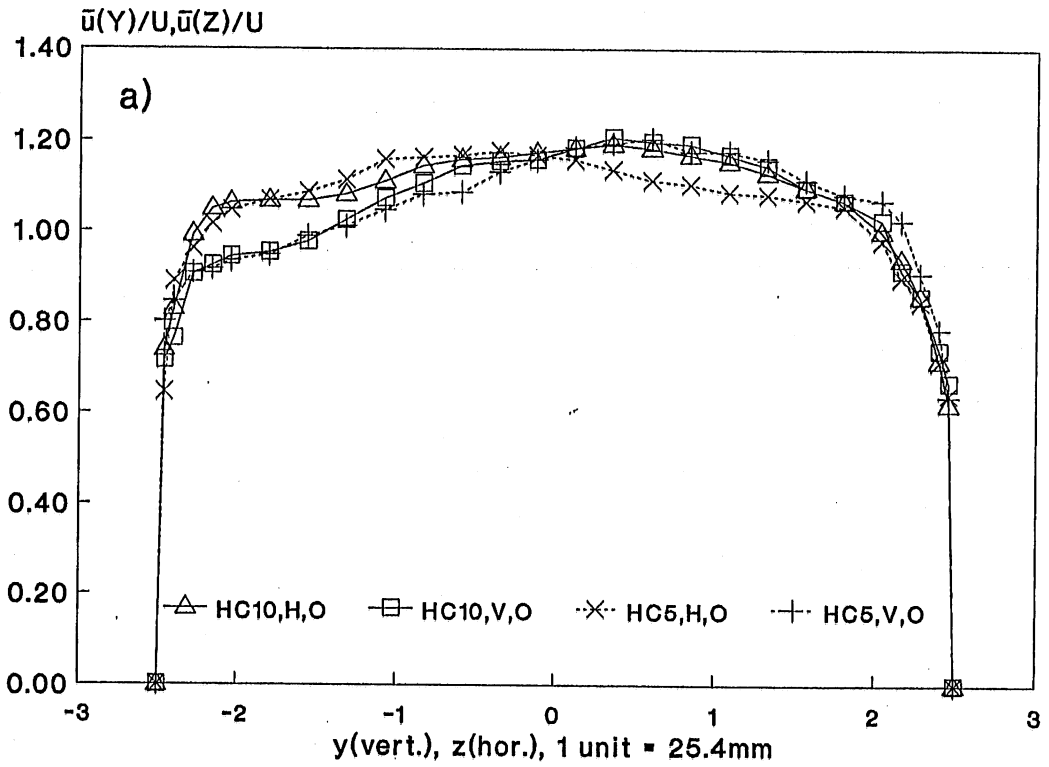

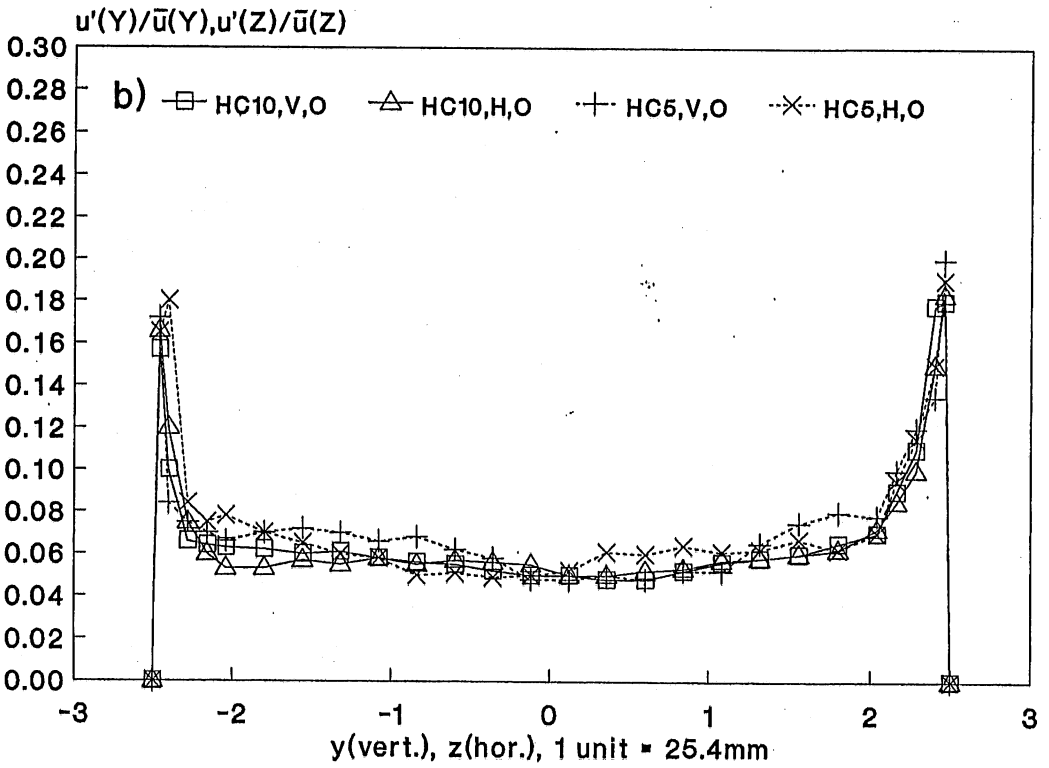

Fig. 6 a) Mean velocity and b) Velocity fluctuation profiles in pipe with honeycomb HC5 and in pipe with honeycomb HC10. Other symbols as in figure 4.

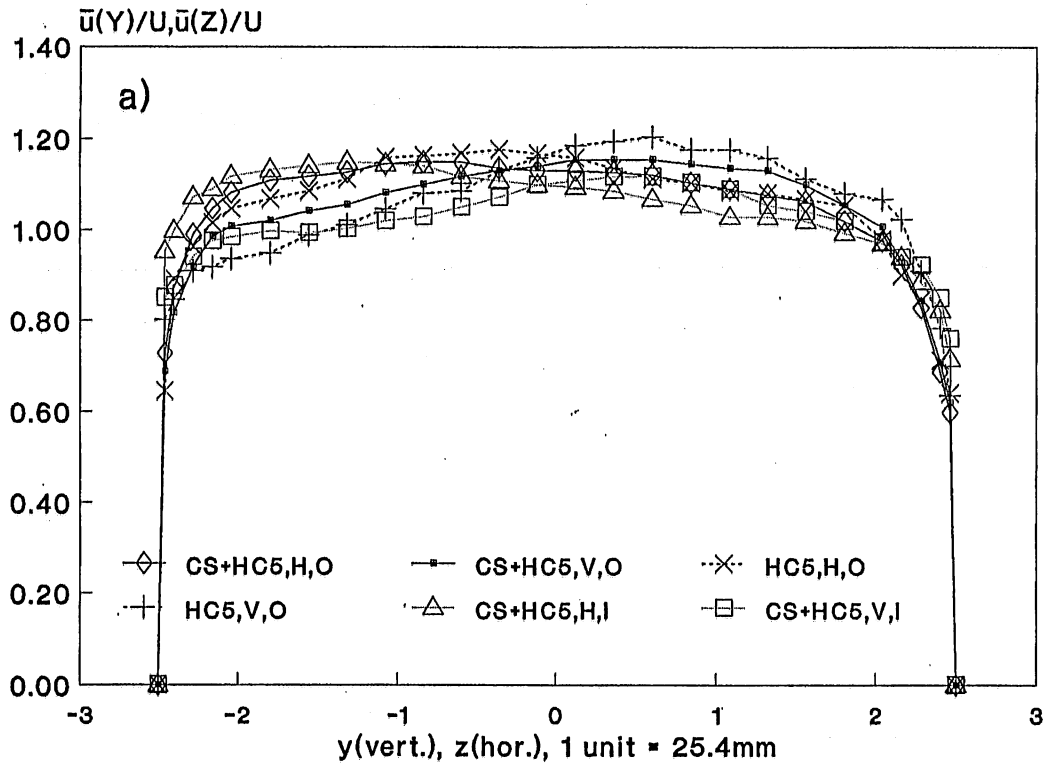

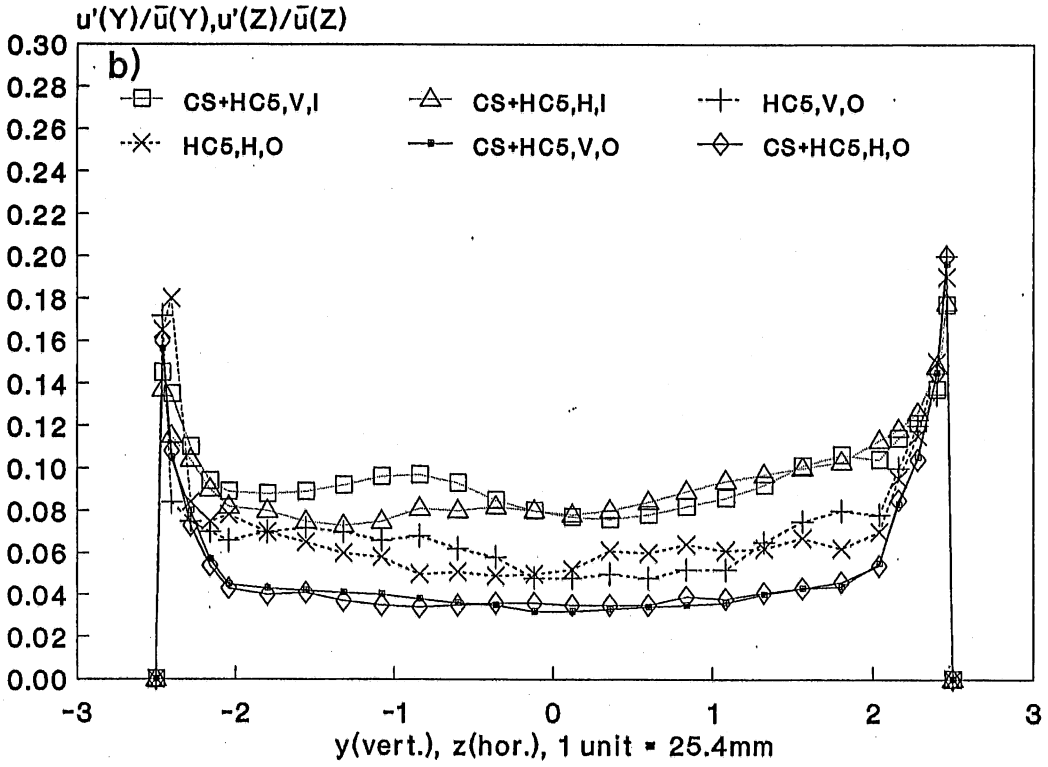

Fig. 7 a) Mean velocity and b) Velocity fluctuation profiles in pipe with honeycomb HC5 and in pipe with coarse screen and honeycomb HC5 (CS+HC5). Other symbols as in figure 4.

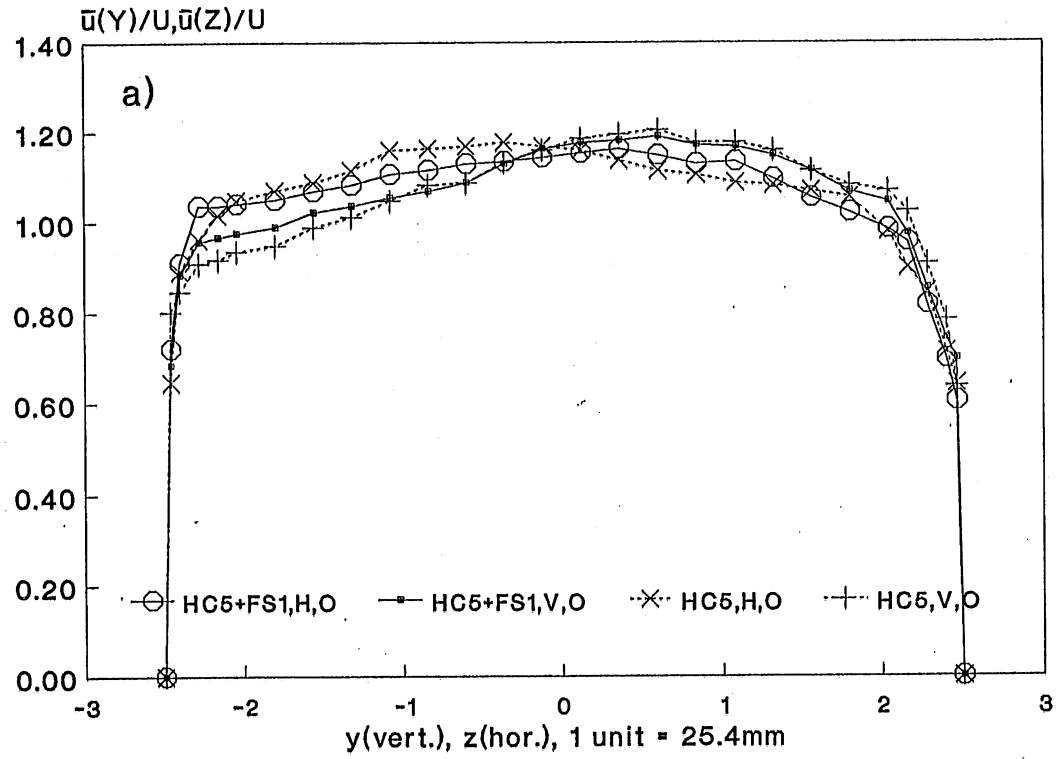

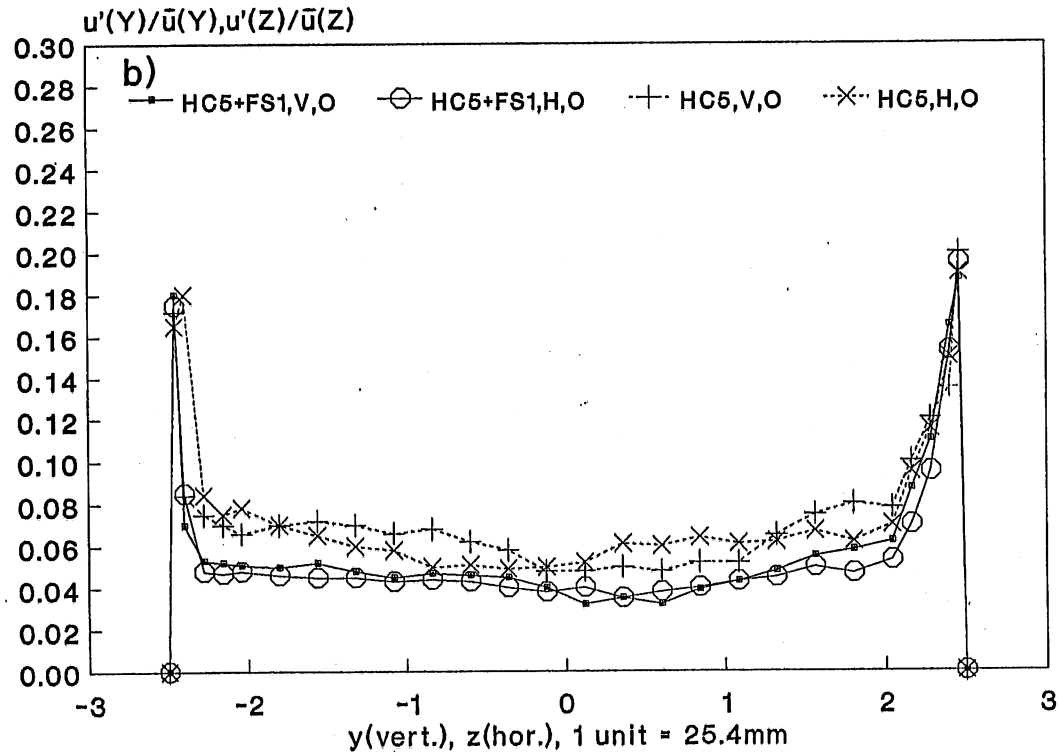

Fig. 8 a) Mean velocity and b) Velocity fluctuation profiles in pipe with honeycomb HC5 and in pipe with honeycomb HC5 and fine screen FS1 (HC5+FS1). Other symbols as in figure 4.

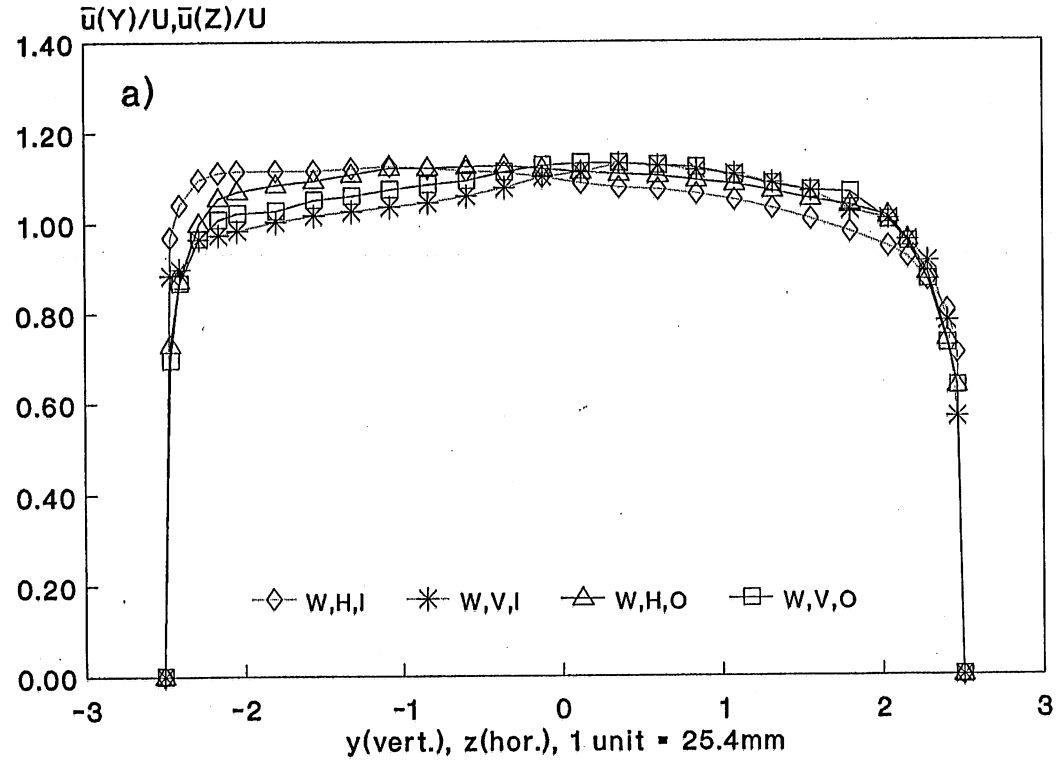

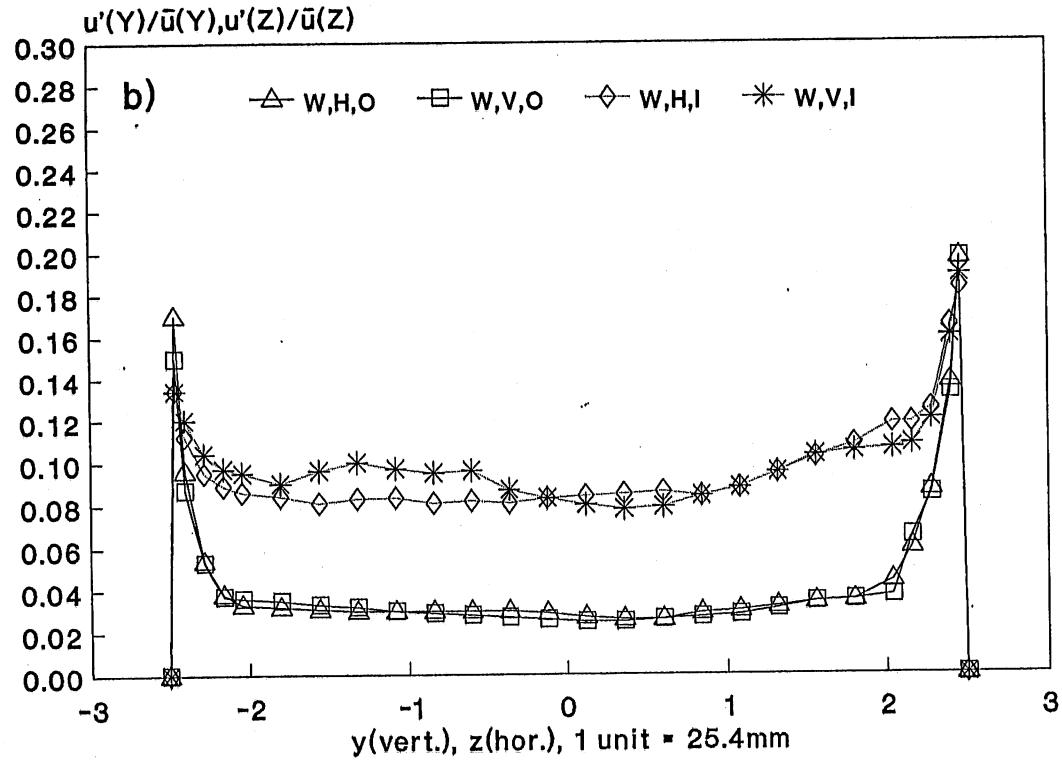

Fig. 9 a) Mean velocity and b) Velocity fluctuation profiles in pipe with coarse screen, honeycomb HC5 and fine screen FS1 (W). Other symbols as in figure 4.

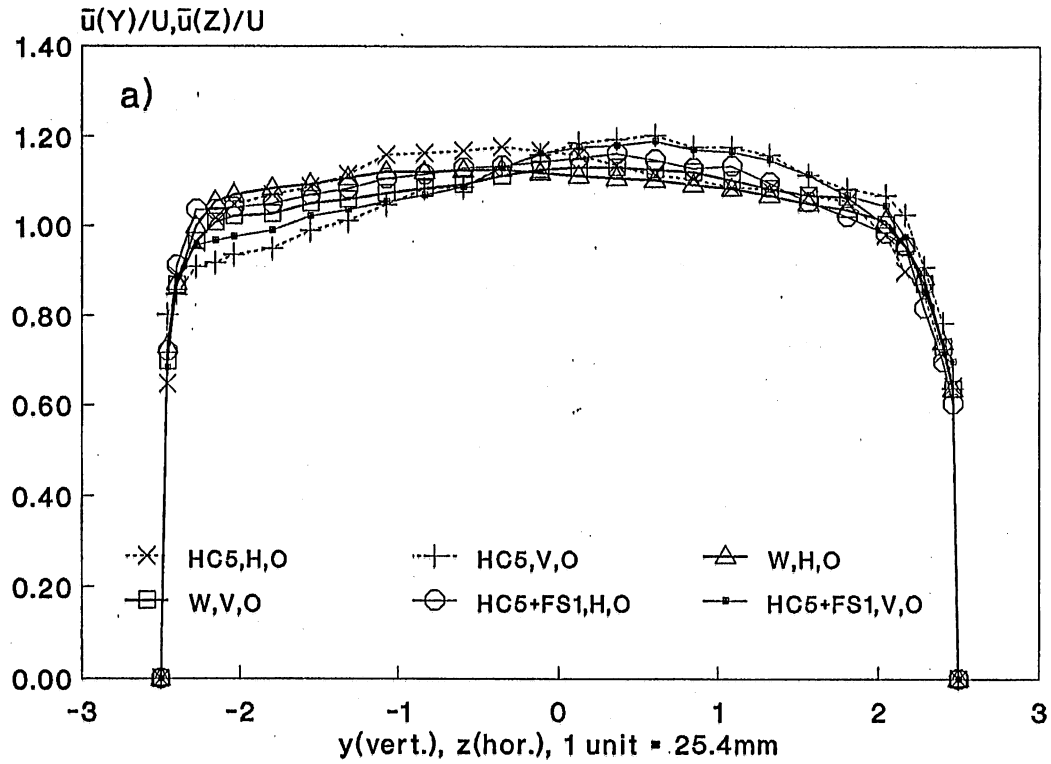

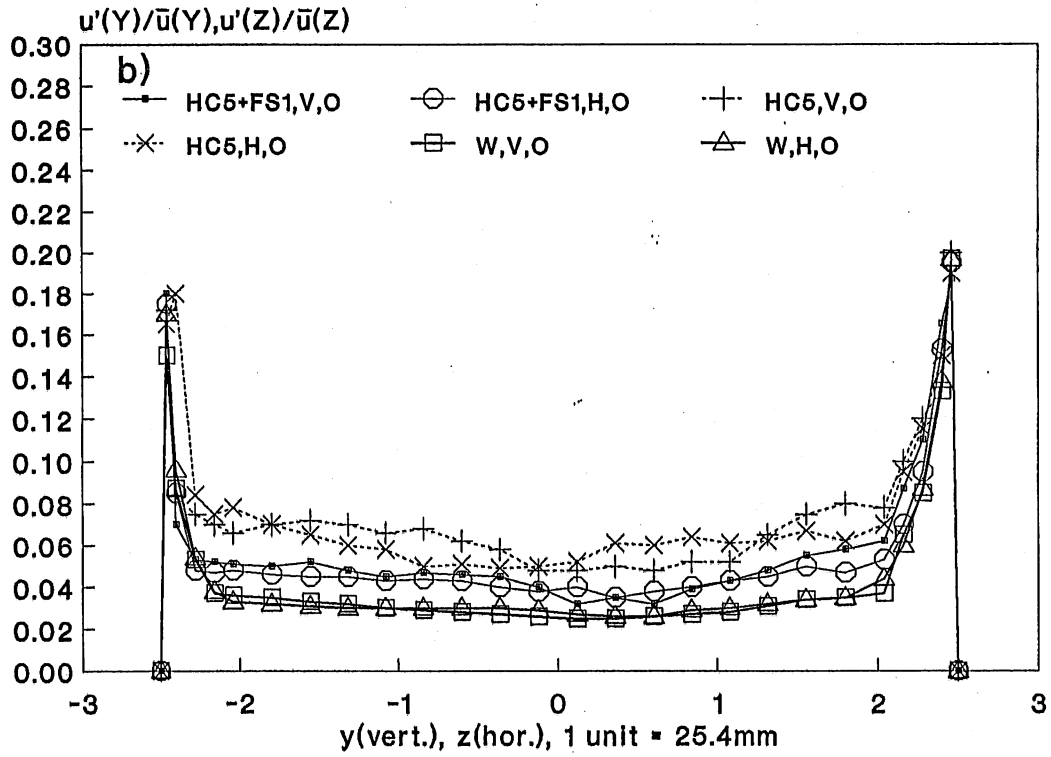

Fig. 10 a) Mean velocity and b) Velocity fluctuation profiles in pipe with honeycomb HC5, in pipe with HC5 and fine screen FS1 (HC5+FS1), and in pipe with coarse screen, HC5 and FS1 (W). Other symbols as in figure 4.

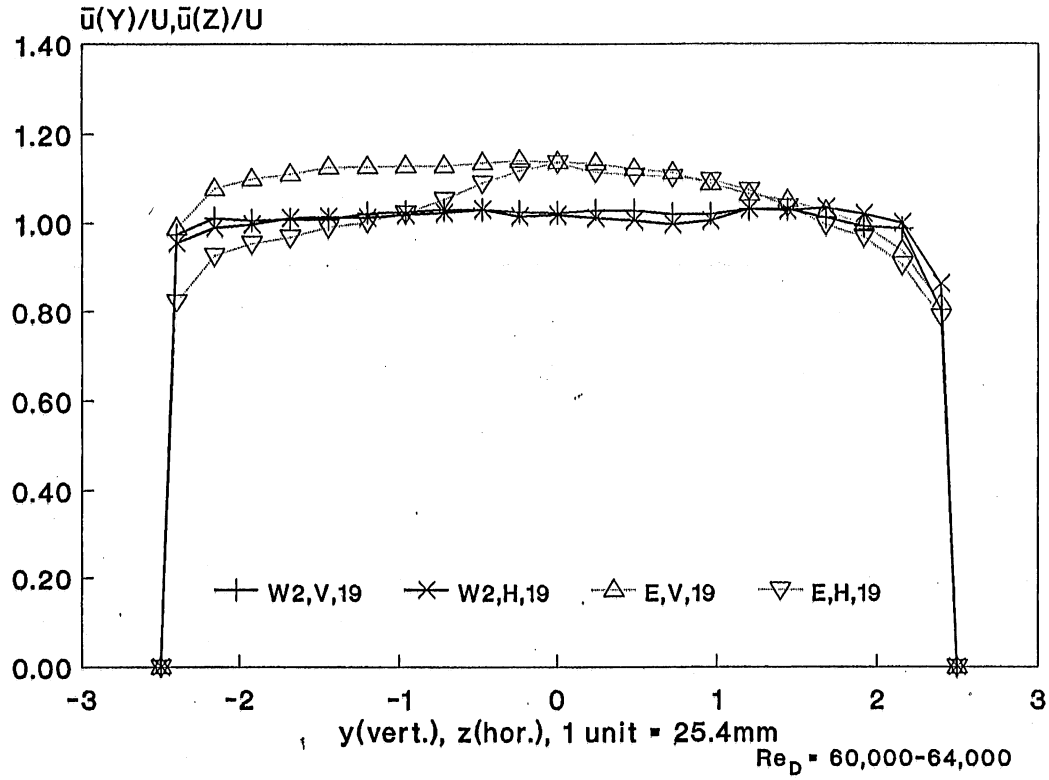

Fig. 11 Mean velocity profiles in empty pipe (E) and in pipe with coarse screen, honeycomb HC5 and fine screens FS1 and FS2 (W2), at distance X = 19 in (482.6 mm). Other symbols as in figure 4.

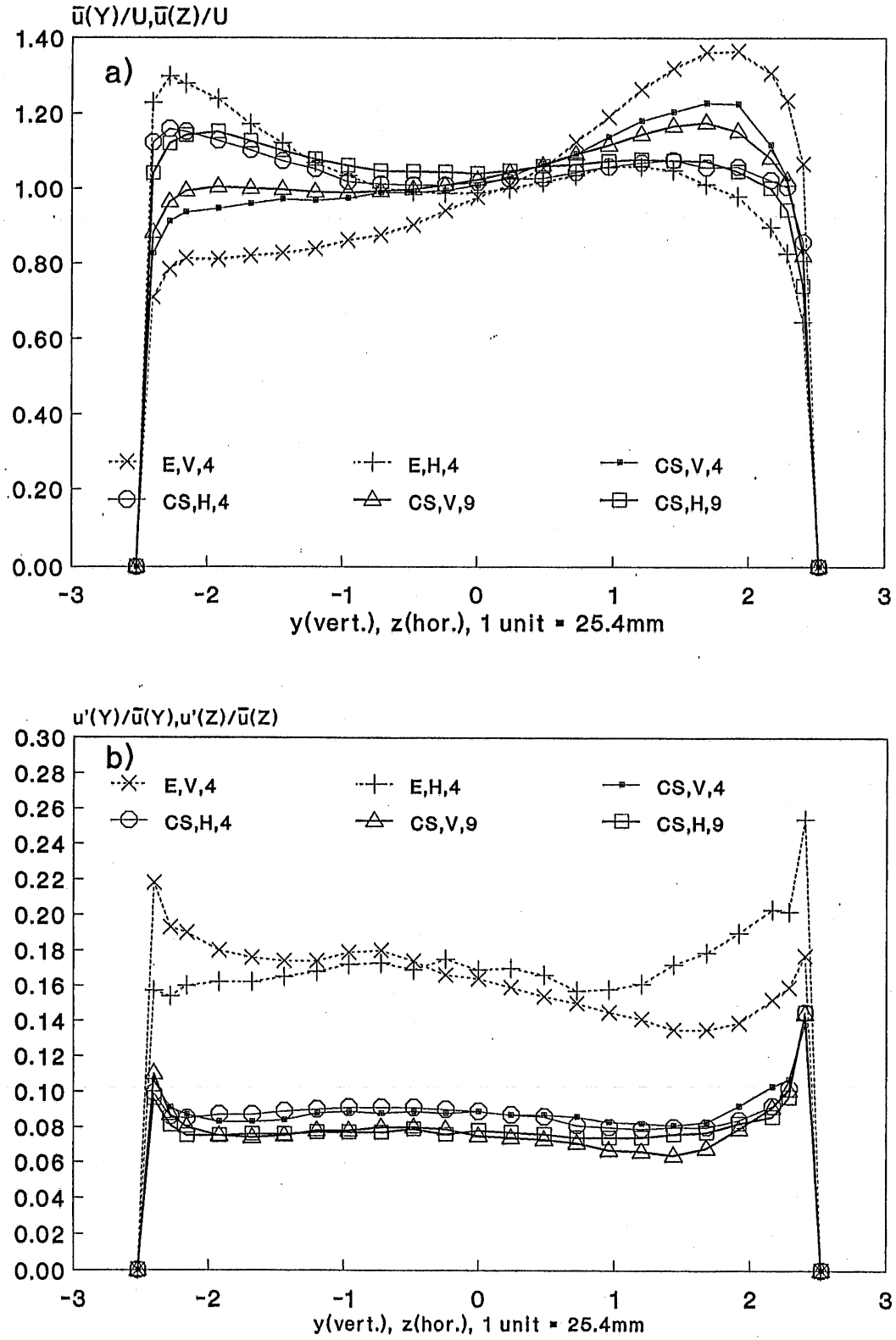

Fig. 12 a) Mean velocity and b) Velocity fluctuation profiles in new facility in empty pipe (E) and in pipe with coarse screen (CS), at distances X = 4 in (101.6 mm) and X = 9 in (228.6 mm). Other symbols as in figure 4.

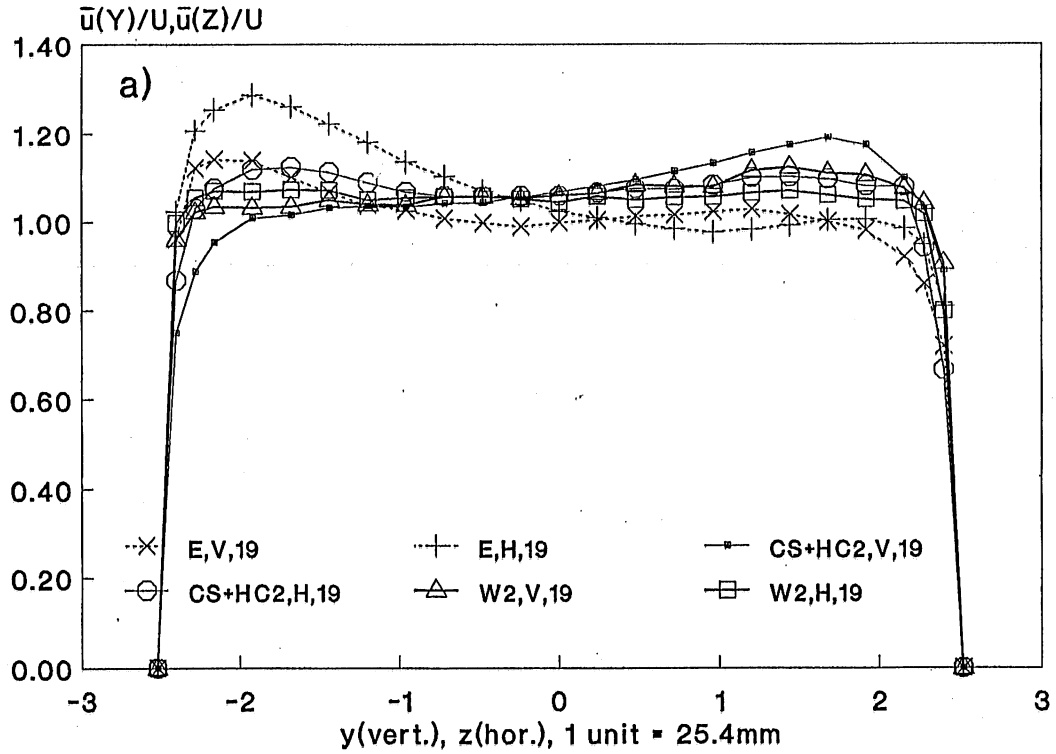

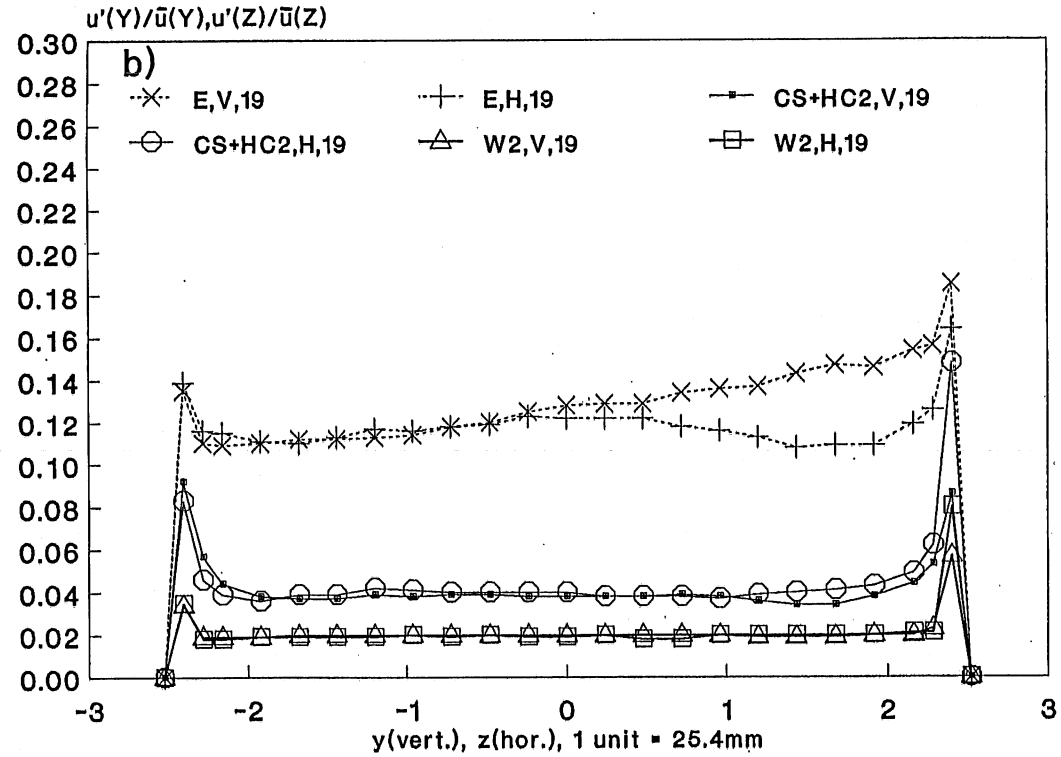

Fig. 13 a) Mean velocity and b) Velocity fluctuation profiles in new facility in empty pipe (E), in pipe with coarse screen and honeycomb HC2 (CS+HC2), and in pipe with CS, HC2, and screens FS1 and FS2 (W2), at distance X = 19 in (482.6 mm). Other symbols as in figure 4.

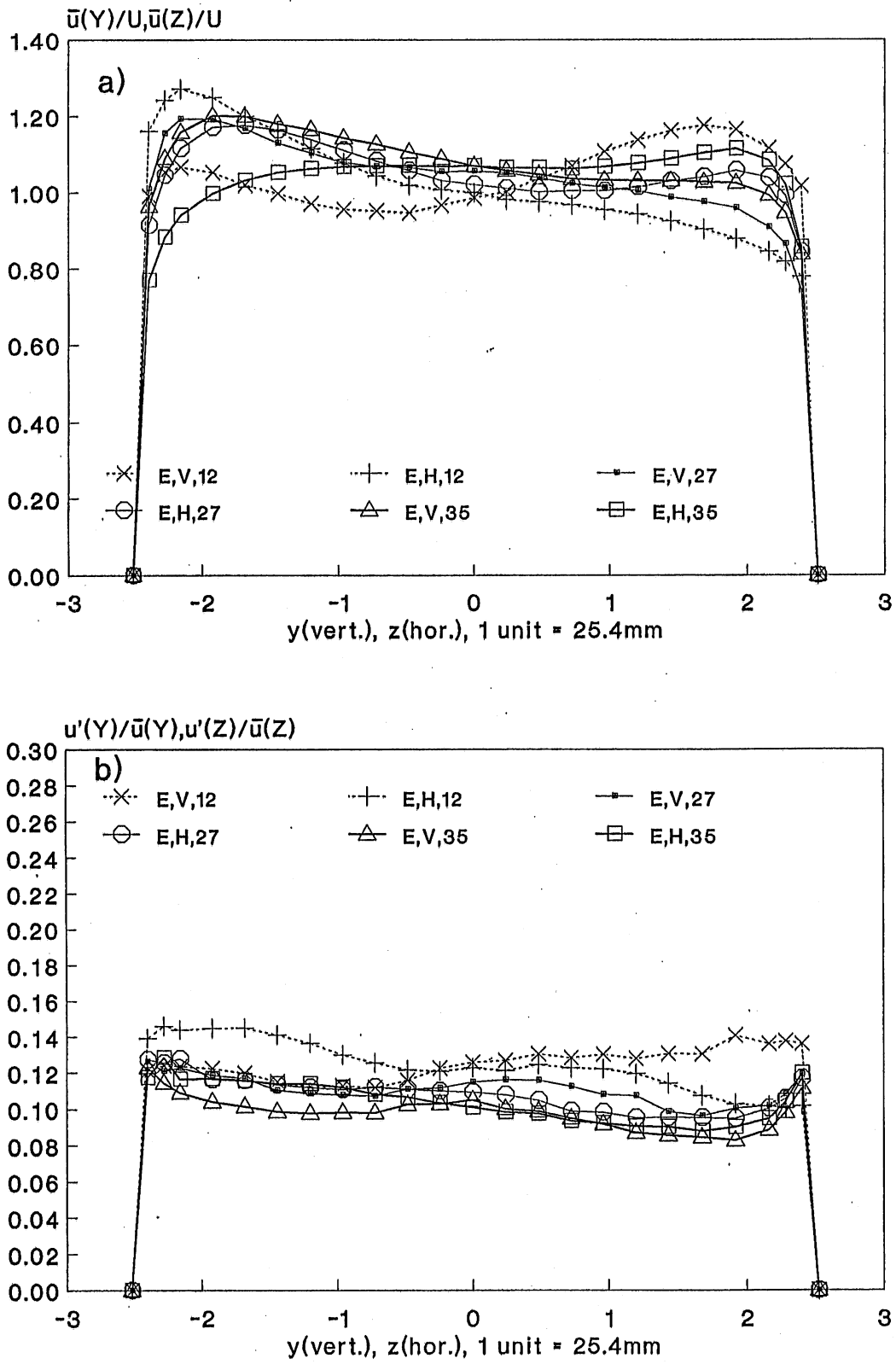

Fig. 14 a) Mean velocity and b) Velocity fluctuation profiles in new facility in empty pipe (E) at distances X = 12 in (304.8 mm), X = 27 in (685.8 mm) and X = 35 in (889 mm). Other symbols as in figure 4.

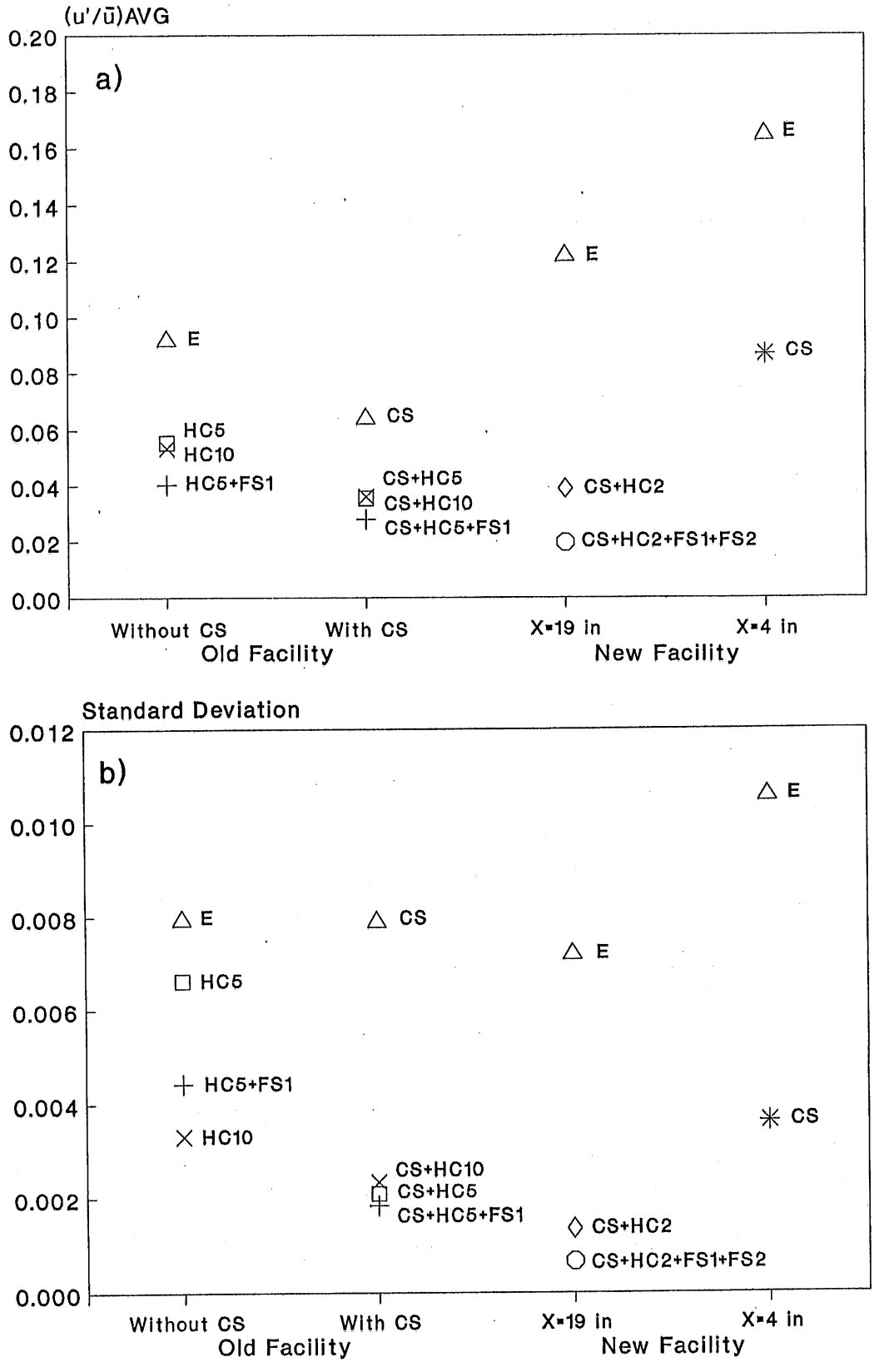

Fig. 15 a) Average and b) Standard deviation of u'/ū values over 55-mm-diameter center portion of the pipe.